Mon. Not. R. Astron. Soc. **382,** 1196–1202 (2007) doi:10.1111/j.1365-2966.2007.12456.x

Anomalous SZ contribution to three-year *WMAP* data

R. M. Bielby★ and T. Shanks
Department of Physics, Durham University, South Road, Durham DH1 3LE

Accepted 2007 September 11. Received 2007 September 3; in original form 2007 April 19

ABSTRACT

We first show that the new *Wilkinson Microwave Anisotropy Probe* (*WMAP*) 3-yr data confirm the detection by Myers et al. of an extended SZ signal centred on 606 Abell (ACO) clusters with richness class, $R \geqslant 2$. Our results also show SZ decrements around APM and 2MASS groups at increased significance than previously detected. We then follow the approach of Lieu, Mittaz & Zhang and compare the stacked *WMAP* results for the decrement in 31 clusters with *ROSAT* X-ray profiles where Lieu et al. found on average less SZ decrement in the *WMAP* 1-yr data than predicted. We confirm that in the 3-yr data these same clusters again show less SZ decrement than the X-ray data predict. We then analysed the *WMAP* results for the 38 X-ray clusters with OVRO/BIMA measured SZ decrements as presented by Bonamente et al.. We again find that the average decrement is measured to be significantly less (5.5σ) than predicted by the *Chandra* X-ray data. Thus while we confirm the original detection of an extended SZ effect by Myers et al., these X-ray comparisons may now suggest that the central SZ amplitudes detected by *WMAP* may actually be lower than expected. One possible explanation is that there is contamination of the *WMAP* SZ signal by radio sources in the clusters but we argue that this appears implausible. We then consider the possibility that the SZ decrement has been lensed away by foreground galaxy groups. Such a model predicts that the SZ decrement should depend on cluster redshift. A reduction in the SZ decrement with redshift is suggested from the ACO cluster sample and also from comparing the samples of Lieu et al. and Bonamente et al.. However, the mass power spectrum would require a far higher amplitude than currently expected if lensing was to explain the SZ deficit in high-redshift clusters.

Key words: galaxies: clusters – cosmic microwave background.

1 INTRODUCTION

Myers et al. (2004) made a cross-correlation analysis between galaxy cluster catalogues and the *Wilkinson Microwave Anisotropy Probe* (*WMAP*) first-year data (Hinshaw et al. 2003). They saw a statistical decrement near groups and clusters as detected by APM and also in more nearby groups and clusters as detected by Two Micron All Sky Survey (2MASS) but the strongest signal was seen in the Abell (ACO)-rich cluster catalogue (Abell, Corwin & Olowin 1989). There the decrement was approximately what was expected from predictions based on X-ray observations of the Coma cluster which is itself a richness class 2 cluster. However, the profile appeared to be more extended than expected from simple fits to these typical cluster X-ray data. The extent of the SZ effect, possibly to $\theta \approx 1^\circ$, led Myers et al. (2004) to speculate whether the SZ effect could contaminate the measurement of the acoustic peaks, although the difference between the SZ and primordial cosmic microwave background (CMB) spectral indices may constrain such a possibility at least for the first peak (Huffenberger, Seljak & Makarov 2004). We now return to this topic with the first aim to see if the extended SZ effect reproduces in the 3-yr *WMAP* data.

Meanwhile, Lieu, Mittaz & Zhang (2006) analysed the *WMAP* first-year data now focusing only on 31 clusters with *ROSAT* X-ray data. They made basic predictions for the SZ decrement in each cluster and found that they overpredicted the SZ decrement. One possibility was that discrete radio sources in the clusters were diluting the decrements but this was argued against by Lieu et al. (2006). However, Lieu & Quenby (2006) suggested an alternative mechanism based on synchrotron radiation from cosmic ray electrons moving in the cluster magnetic field forming a diffuse cluster radio source which again may dilute the SZ effect. This model was also aimed at explaining the soft X-ray excesses detected in some clusters via inverse Compton scattering of the CMB by the same cosmic ray electrons in the cluster (e.g. Nevalainen et al. 2003 and references therein).

Here we shall check the result of Lieu et al. (2006) using our cross-correlation methodology and the full *WMAP* 3-yr data. In the first instance, we shall take the X-ray models of Lieu et al. (2006) which follow the simple β model prescription described in Section 3

★E-mail: r.m.bielby@durham.ac.uk

below. We shall also look at a new sample of clusters with excellent *Chandra* X-ray data (Bonamente et al. 2006). Again we shall simply take their models convolved for the *WMAP* point spread function in the appropriate band and compare to the averaged SZ decrement seen in the *WMAP*3 data.

2 DATA

2.1 *WMAP* third-year data

In this paper we use the raw CMB temperature maps provided in the *WMAP* 3-yr data release (Hinshaw et al. 2006). These consist of temperature data from the five frequency bands and the internal linear combination (ILC) map (Table 1). In order to remove contamination from our own Galaxy, we make use of the Kp0 foreground mask made available with the other *WMAP* data products and have applied this to all our maps prior to cross-correlation. Finally, the data are used here in the HEALPix format of equal-area data elements, characterized by $N_{side} = 512$, which gives an element width of ≈7 arcmin.

2.2 Cluster data

2.2.1 ACO

The ACO catalogue (Abell et al. 1989) lists clusters with 30 or more members, given the requirements that all members are within 2 mag of the third brightest cluster member, whilst also lying within a 1.5 h^{-1} Mpc radius. A richness class, R, is applied to the individual clusters based on a scale of $0 \leqslant R \leqslant 5$. The catalogue covers both hemispheres and here we trim these samples such that we take clusters of only $R \geqslant 2$ and galactic latitudes of $|b| \geqslant 40^\circ$.

2.2.2 APM

We shall also use galaxy group and cluster catalogues derived from the APM Galaxy Survey of Maddox et al. (1990) which covers the whole area with $\delta < -2.^\circ5$ and $b < -40^\circ$. These were identified using the same 'friends-of-friends' algorithm as Myers et al. (2003) and references therein. Circles around each APM galaxy with $B < 20.5$ are 'grown' until the overdensity, σ, falls to $\sigma = 8$ and those galaxies whose circles overlap are called groups. The APM galaxy surface density is $N \approx 750\,\mathrm{deg}^{-2}$ at $B < 20.5$. Minimum memberships, m, of $m \geqslant 7$ and $m \geqslant 15$ were used. The sky density of groups and clusters is $3.5\,\mathrm{deg}^{-2}$ at $m \geqslant 7$ and $0.35\,\mathrm{deg}^{-2}$ at $m \geqslant 15$. We assume an average redshift of $z = 0.1$ for both APM samples.

2.2.3 2MASS

The third cluster catalogue is derived from the final data release of the 2MASS Extended Source Catalogue (Jarrett et al. 2000) to a limit of $K_s \leqslant 13.7$. K-selected galaxy samples are dominated by early-type galaxies which are the most common galaxy type found in rich galaxy clusters. Therefore the 2MASS survey provides an excellent tracer of the high-density parts of the Universe out to $z < 0.15$ and so provides a further test for the existence of the SZ effect. Using the above 2D friends-of-friends algorithm, Myers et al. (2004) detected 500 groups and clusters with $m \geqslant 35$ members at the density contrast $\sigma = 8$ in the $|b| \geqslant 10^\circ$ area. The 2MASS groups have average redshift, $z \approx 0.06$.

Table 1. Properties of the *WMAP* frequency bands.

Band	Frequency (GHz)	FWHM (arcmin)
W	94	12.6
V	61	19.8
Q	41	29.4
Ka	33	37.2
K	23	49.2

2.2.4 ROSAT X-ray cluster sample

The 31 clusters published by Bonamente et al. (2002) were originally selected as a sample of X-ray bright clusters suitable for observing X-ray surface brightness profiles. These profiles were obtained with the *ROSAT* PSPC instrument and estimates of the gas temperature, density and distribution were made by fitting a β profile model to the data (see Section 3 below). The X-ray data for these 31 clusters were previously used by Lieu et al. (2006) to construct predictive models of the SZ profile of each cluster. Redshifts for the clusters range from $z \sim 0.02$ (Coma) up to $z \sim 0.3$ (Abell 2744), whilst the sample lies in the galactic latitude range of $|b| \geqslant 25^\circ$.

2.2.5 Chandra X-ray cluster sample

We further analyse the 38 clusters discussed by Bonamente et al. (2006). These clusters have been observed at 30 GHz by OVRO and BIMA (see Bonamente et al. (2006) and references therein) to detect the SZ decrements and have also been observed by *Chandra* to provide the X-ray data needed to estimate the value of H_0. The interferometric radio observations have a resolution of ≈1 arcmin and the X-ray observations from the *Chandra* ACIS-I camera have a resolution of ≈1 arcsec. Redshifts for these clusters are in the range $0.18 < z < 0.8$, a higher range than for the *ROSAT* sample. Bonamente et al. (2006) fitted both hydrostatic equilibrium and isothermal β models to the X-ray data and made predictions for the SZ decrements.

3 SZ X-RAY MODELLING

The SZ effect is generally modelled using X-ray gas profiles, densities and temperatures. The X-ray data are most simply modelled by fitting a β model to the X-ray intensity profile:

$$S_X = S_{X0}\left(1 + \frac{\theta^2}{\theta_c^2}\right)^{(1-6\beta)/2}, \quad (1)$$

where S_{X0} is the central X-ray surface brightness and θ_c is the angular core radius. On the isothermal assumption, the temperature decrement, ΔT_{SZ}, as a function of the angular distance from the cluster centre, θ, is then given by

$$\Delta T_{SZ}(\theta) = \Delta T_{SZ}(0)\left[1 + \left(\frac{\theta}{\theta_c}\right)^2\right]^{-3\beta/2+1/2}. \quad (2)$$

Then the magnitude of the central temperature shift, $\Delta T_{SZ}(0)$, is given by

$$\frac{\Delta T_{SZ}(0)}{T_{CMB}} = \frac{kT_e}{m_e c^2}\sigma_{Th}\int \mathrm{d}l \quad n_e\left[\frac{x(e^x+1)}{e^x-1} - 4\right] \quad (3)$$

where $x = h\nu/kT_e$, σ_{Th} is the Thomson cross-section and n_e, T_e are the gas density and temperature derived from the X-ray data.

Lieu et al. (2006) use the cluster sample of Bonamente et al. (2002) and fit *ROSAT* PSPC cluster X-ray profiles. They assume isothermal gas distributions with T_e taken from Bonamente et al. (2002). Bonamente et al. (2006) use both a hydrostatic equilibrium model, allowing a double power law β model to allow for variations in the number density with radius, and an isothermal β model. With the hydrostatic model, they allow the gas temperature to vary with radius and a cold dark matter component as well as gas to contribute to the cluster potential. We shall simply assume the isothermal models of Lieu et al. (2006) and Bonamente et al. (2006) and convolve the predicted SZ profile with the appropriate *WMAP* beam profile, modelled as a Gaussian with the full width at half-maximum (FWHM) beamwidths shown in Table 1.

4 CROSS-CORRELATION ANALYSIS

We focus our analysis on the 94-GHz *W* band from *WMAP*, looking for correlations characteristic of the SZ effect in this, the highest resolution band. We perform a cross-correlation analysis as described in Myers et al. (2004), calculating the mean temperature decrement/increment as a function of angular separation from galaxy clusters in the above data sets. Our cross-correlation takes the form

$$\Delta T_c(\theta) = \sum_i \frac{\Delta T_i(\theta) - \overline{\Delta T}}{n_i(\theta)}, \quad (4)$$

where $\Delta T_i(\theta)$ is the *WMAP* temperature in an element i at an angular separation θ from a cluster centre and n_i is the number of elements at that separation. $\overline{\Delta T}$ is the mean *WMAP* temperature decrement across the entire region used in the analysis. For the 3-yr *W*-band data, $\overline{\Delta T} \sim 10^{-3}$ mK.

Errors on our results are estimated using repeated Monte Carlo realizations of the cluster data. As each catalogue (i.e. 2MASS, ACO, APM) will each be highly clustered, it is important to incorporate this clustering into the realizations. Thus for each realization we begin by creating a set of random positions with 5× the number of clusters as in the parent catalogue. We then calculate a clustering amplitude for each individual cluster in this random sample and attribute a weighting based on the assigned clustering amplitude. Clusters are then selected or discarded based on this weighting, until the realization has the required number of selected clusters (i.e. that of the parent catalogue). As a final check, the autocorrelation of the realization is measured. Through comparison with the autocorrelation of the original catalogue, the realization is either accepted or discarded. This process is repeated until we have 100 acceptable clustered mock catalogues for each parent catalogue. The cross-correlation is then calculated between the *WMAP* data and the 100 mock catalogues and the standard deviation is taken as the 1σ error on our results.

In addition to this we also perform a rotational analysis to provide an alternative estimate of the errors. In this case we perform the cross-correlation between the cluster positions and the *WMAP* data. We then shift the cluster positions by 20° in galactic longitude and recalculate the cross-correlation. We repeat this until we have rotated through a full 360°. A signal-to-noise ratio (S/N) is then calculated from the results of this rotational analysis.

5 RESULTS

5.1 Optical/IR cluster samples

The results for the cross-correlation between the four large cluster data sets (APM $m \geqslant 7$, APM $m \geqslant 15$, ACO $R \geqslant 2$ and 2MASS clusters) and the *WMAP W*-band data are shown in Fig. 1. A decrement is immediately evident on small scales within $\theta < 30$ arcmin of cluster centres in all four data sets. Looking in detail first at the ACO results, the *WMAP*3 cross-correlation strongly confirms the results of Myers et al. (2004) from *WMAP* first-year data. Here, we find a decrement of -0.021 ± 0.007 mK at $\theta < 6.3$ arcmin and -0.010 ± 0.004 mK at $\theta < 60$ arcmin for the *W*-band data (quoted accuracies are from the Monte Carlo analysis). Basically, the ACO decrement has remained the same and the improved statistics at small angles has increased the S/N. In addition to the Monte Carlo analysis, we also checked our ACO results using the rotational analysis described by Myers et al. (2004) and find the significance of the decrement at 6.3, 60 and 500 arcmin to be $3.2\sigma, 2.0\sigma$ and 1.2σ (see Fig. 2). As before, there appears to be some form of extended signal out to angles of ∼100 arcmin. Following Myers et al. (2004), we also produce the correlations with the four other *WMAP* bands, plus the ILC map. The results of this are shown in Fig. 3. Again, good agreement is seen between these updated results and the original first-year data results. Despite the increasingly poor resolution of the bands, the decrement is observed in the *V*, *Q* and *Ka* bands, whilst even the ILC map and the *Ka* band map show a decrement.

Improvements in the small scale statistics are also observed in the 2MASS and APM results while the magnitudes of the decrements remain unchanged. However, the APM group ($m \geqslant 7$) SZ detections remain marginal even at small scales.

5.2 *ROSAT* X-ray bright cluster sample

We next consider the X-ray bright clusters of Bonamente et al. (2002). Analysis of this data set with respect to the first-year *WMAP*

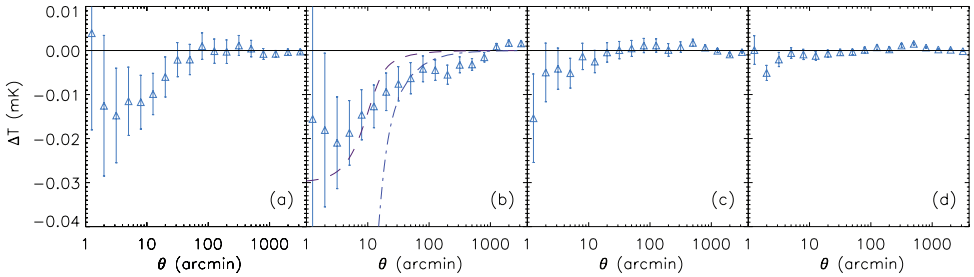

Figure 1. Cross-correlation results between the *WMAP* 3-yr *W*-band temperature data and the four cluster data sets: (a) 2MASS, (b) ACO, (c) APM $m \geqslant 15$ and (d) APM $m \geqslant 7$. The dashed and dot–dashed lines in (b) show SZ models with $\Delta T = 0.083$ and 0.49 K, respectively, both with $\theta_c = 1.5$ arcmin and $\beta = 0.75$ and convolved with the *WMAP* beamwidth. The latter model is intended to be representative of the Coma cluster, scaled to redshift $z = 0.15$. The former is the ACO model fitted by Myers et al. (2004) in their analysis of the *WMAP* first-year results.

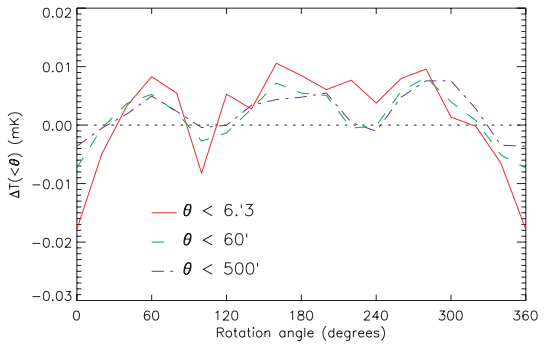

Figure 2. The cross-correlation of the ACO catalogue is shown after increments in galactic longitude of 20° in the Abell cluster positions. The mean ΔT is shown for *WMAP* pixels within 6.3, 60 and 500 arcmin of cluster centres, where the significance at each angular limit is 3.2, 2.0 and 1.2σ, respectively.

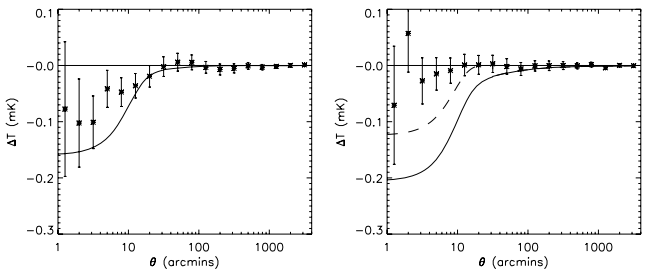

Figure 4. Average ΔT (from *WMAP W*-band data) plots for 30 clusters from the *ROSAT* sample (left-hand panel) and 39 clusters from the *Chandra* sample (right-hand panel). In both figures, the points show our cross-correlation results, whilst the curves show average SZ models (based on the parameters taken from Lieu et al. 2006 and Bonamente et al. 2006) convolved with a Gaussian representing the *WMAP* beam profile. For the *Chandra* sample, we plot the full isothermal model (solid line) and the same model limited to $\theta < 2$ arcmin (dashed line).

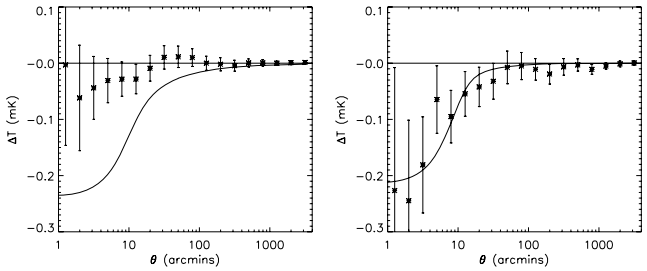

Figure 5. Average ΔT (from *WMAP W*-band data) correlations for the *ROSAT* X-ray clusters split by redshift: 21 clusters at $z < 0.1$ (left-hand panel) and nine at $z > 0.1$ (right-hand panel).

results has already been performed by Lieu et al. (2006). Their main conclusion was that the SZ decrement in the *WMAP*1 data around the locations of these clusters has a lower magnitude than they would expect from their predictions based on the original X-ray observations of Bonamente et al. (2002). In Fig. 4 (left-hand panel) we show our cross-correlation between the 31 clusters used by Lieu et al. (2006) and the *WMAP* year 3 data in the *W* band (crosses). We also present the average model prediction based on the Bonamente et al. (2002) data (solid line). This has been convolved with a Gaussian beam profile of $\sigma = 6.3$ arcmin. We see the same general effect as seen by Lieu et al. (2006), that the SZ effect is somewhat smaller than predicted by the data. However, the significance of rejection is only $\approx 2\sigma$. Similar results are seen in the other *WMAP* bands.

We next split the Lieu et al. (2006) clusters by redshift as shown in Fig. 5. Again our results are given by the crosses, whilst the solid lines show the average model SZ profiles. The model for clusters at $z < 0.1$ is rejected by 4.2σ at $\theta < 6.3$ arcmin, whilst at $0.1 < z < 0.3$ the rejection drops to 1.6σ at $\theta < 6.3$ arcmin. We have also performed this analysis with a latitude split at $|b| = 40°$ and find some degeneracy between latitude and redshift as many of the low-redshift clusters are also at low latitude. However, in either case

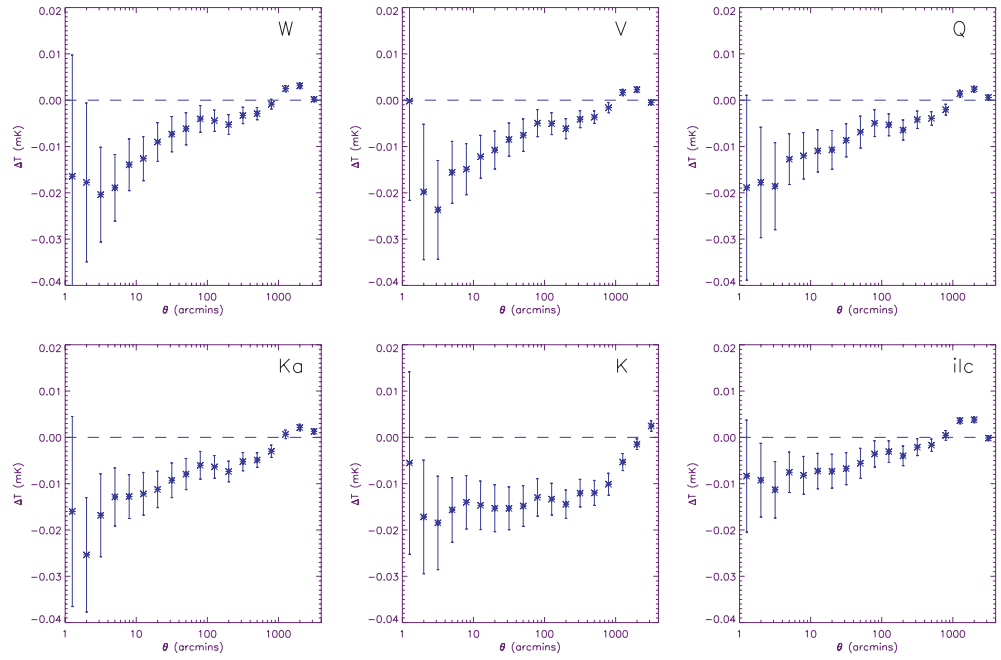

Figure 3. Cross-correlation results between 606 ACO-rich galaxy clusters ($R \geqslant 2$, $|b| > 40°$) and the *WMAP* 3-yr maps in five bandpasses (+ILC) as indicated.

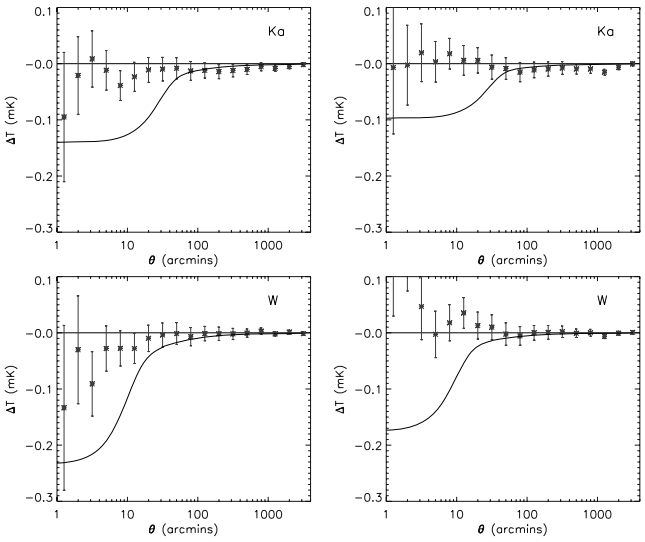

Figure 6. Top: Cross-correlations of *WMAP Ka*-band ΔT data with 20 clusters at $z < 0.3$ (left-hand panels) and 19 at $z > 0.3$ (right-hand panels) from the *Chandra* cluster sample. Bottom: The same for *WMAP W*-band data. The solid lines show the β models of Bonamente et al. (2006) convolved with the *WMAP* profiles.

we do not regard the difference between the results in Fig. 5 as particularly statistically significant.

5.3 *Chandra* X-ray bright cluster sample

We next analysed the SZ decrements for the 38 clusters of Bonamente et al. (2006), using the *WMAP*3*W*-band results. In Fig. 4 (right-hand panel) we compare the cross-correlation results with an average model constructed from the individual isothermal models given in table 5 of Bonamente et al. 2006 (solid line) and again find that the SZ effect is now quite severely overpredicted by the models, with a rejection significance of 5.5σ. We again looked for a dependence on redshift and found slight evidence for a greater SZ signal at $z < 0.3$ compared to $z > 0.3$ (Fig. 6).

Given that Bonamente et al. (2006) only fit the *Chandra* data for $\theta < 2$ arcmin, there is the possibility that this model may not apply at the large angles covered by the *WMAP* data. We therefore also show in Fig. 4 the SZ model truncated at $\theta = 2$ arcmin before being convolved with the *W*-band beam (dashed line). The significance of rejection in this case is reduced to 2.5σ. We note that this is a strict lower limit to this significance limit as it assumes no SZ contribution beyond 2 arcmin.

Although within the *Chandra* sample there is little evidence of redshift dependence, the fits of SZ models to the *WMAP* data do appear to deteriorate as we move from the average redshift, $z \approx 0.1$ of the *ROSAT* sample to $z \approx 0.3$ of the *Chandra* sample (Fig. 4). We have also noted that at the lowest redshift the *WMAP* SZ effect is clearly detected at about the predicted amplitude in the Coma cluster (Fig. 7). We therefore returned to the ACO data set and identified 407 $R \geqslant 2$, $|b| > 40^\circ$ clusters with measured redshifts. Splitting these at $z = 0.15$ (Fig. 8), we see that there is some evidence confirming that clusters at higher redshift have observed SZ decrements that are significantly smaller than at lower redshift. Although the X-ray properties for the majority of these clusters are unknown, we have fitted the same average model, scaling θ_c to the appropriate average redshift before convolving with the *WMAP* beam. The fit appears significantly worse for the higher redshift clusters, with a

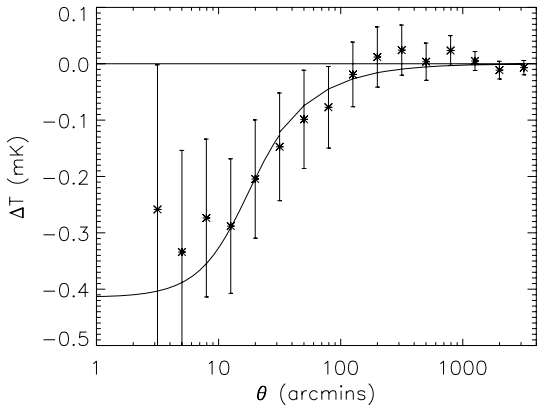

Figure 7. Binned ΔT data from the *WMAP* yr-3 *W*-band data around the Coma cluster. The solid line shows the model predicted from X-ray data (taken from Lieu et al. 2006) convolved with the *W*-band beam profile.

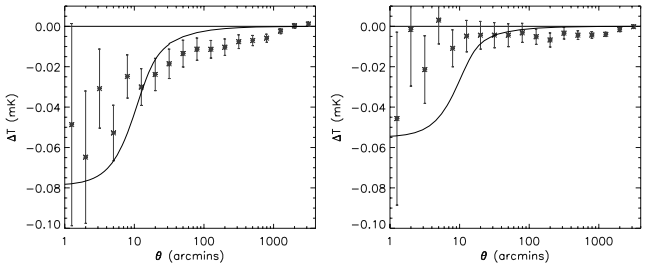

Figure 8. Average ΔT (from *WMAP W*-band data) plots for the data from the Abell cluster catalogue with 172 clusters at $z < 0.15$ (left-hand panel) and 235 at $z > 0.15$ (right-hand panel). Only clusters with $|b| \geqslant 40^\circ$ are included here. Overlaid in both cases is a model with $\Delta T(0) = -0.16\,mK$, $\beta = 0.7$ and $\theta_c = 9.8$ arcmin scaled to the mean redshift of the samples: $z = 0.1$ and 0.2. In both cases the model is convolved with the *W*-band beam profile. This model gives a reasonable fit to the data at $z < 0.15$, but significantly overestimates the $z > 0.15$ data.

rejection confidence at $\theta < 6.3$ arcmin of $\approx 1\sigma$ for $z < 0.15$ and $\approx 4\sigma$ for $z > 0.15$. We tentatively conclude that there may be a redshift dependence of the SZ effect in the sense that higher redshift clusters show a smaller than expected effect.

6 DISCUSSION

The reduced SZ decrements in the *WMAP*3 data towards the *ROSAT* cluster sample and the almost lack of detection of the SZ effect in terms of the Bonamente et al. (2006) clusters is paradoxical. The most obvious explanation is that the *WMAP* data are contaminated by unresolved cluster radio sources within the *WMAP* beam. However, the contamination from synchrotron radio point sources varies with frequency as $T_\nu \propto \nu^{\alpha-2}$ (where $\alpha \approx 0.7$), whilst the discrepancy in the *WMAP*3 data for the Bonamente et al. (2006) cluster sample is as large at *Ka* (33 GHz) as at *W* (94 GHz) (see Fig. 6).

Further to this issue, we note that a survey of radio sources in the *Chandra* clusters has been performed by Coble et al. (2007). They see a population of radio sources with a mean flux of ≈6.2 mJy per cluster at 30 GHz. Given a spectral index of such sources of $\alpha \approx 0.7$ (where $S_\nu \propto \nu^{-\alpha}$) this gives a flux of ≈3 mJy per cluster at the *W*-band frequency of 90 GHz. Following Lieu et al. (2006), the equivalent flux required to cause the lack of SZ effect observed in the *Chandra* clusters can be determined from the Rayleigh–Jeans

flux multiplied by the solid angle

$$S_{\rm SZ} = \frac{2\pi k \Delta T \nu^2}{c^2} \frac{\theta^2}{4}. \quad (5)$$

Taking $\Delta T = 0.1$ mK, $\nu = 90$ GHz and $\theta = 10$ arcmin, we obtain a flux of $S_{\rm SZ} = 170$ mJy. Even taking a value for the spectral index of $\alpha = 0$ for the radio sources (e.g. Bennett et al. 2003), the flux required is over an order of magnitude greater than the observed discrete radio source fluxes from Coble et al. (2007). In addition, Lin & Mohr (2007) make estimates of the contamination from radio point sources and for cluster masses typical of the *Chandra* sample ($M_{200} \sim 10^{15}\,{\rm M}_{\odot}$, Reiprich & Böhringer 2002), they suggest that up to only 10 per cent of these clusters may be lost due to point source radio contamination (see their fig. 15). Although this assumes that there will be no increase in source contamination with the *WMAP* beam area, we note that the counts of Coble et al. (2007) are usually lower than predicted by Lin & Mohr (2007, fig. 13) and these effects may cancel.

Currently we have no explanation for the strong SZ decrements detected by the interferometric experiments as opposed to the lack of detections by *WMAP*. At higher resolution it may be more possible to detect the SZ against the noise caused by the primordial CMB fluctuations but our error analysis should take care of such statistical effects and the average model is rejected at the 5.5σ level by the *WMAP* data. A high value of $H_0 \approx 100\,{\rm km\,s^{-1}\,Mpc^{-1}}$ for the SZ X-ray model might help explain the *ROSAT* cluster results but an even higher value would be required to explain the *Chandra* cluster results.

As noted above there may also be evidence that the SZ decrement is too low in the ACO–*WMAP*1 cross-correlation of Myers et al. (2004), as confirmed by the ACO–*WMAP*3 cross-correlation in Fig. 1. Myers et al. (2004) noted that the decrement that fitted the ACO $R \geqslant 2$ clusters with $\beta = 0.75$ was only $\Delta T(0) = 0.083$ mK compared to the 0.5 mK predicted for the $R = 2$ Coma cluster. The *WMAP*3 data confirm that $\Delta T(0) = 0.5$ mK is needed to fit the observed Coma SZ decrement (see Fig. 7). In Fig. 1 the SZ models for these two values of the decrement are compared to the *WMAP*3 *W*-band data for the $R \geqslant 2$ cluster sample. Both models assume $\beta = 0.75$. We see that while the data are well fitted at $\theta < 10$ arcmin by the $\Delta T(0) = 0.083$ mK model, the $\Delta T(0) = 0.5$ mK at least begins to improve the fit at larger scales. One possibility is that, as well as detecting an extended SZ component to the ACO data, we may actually be detecting a lower central SZ amplitude than expected from the X-ray data.

Lieu et al. (2006) discussed other possible explanations for the unexpectedly small SZ decrements detected in the *ROSAT* sample. For example, Lieu & Quenby (2006) have discussed whether a diffuse cluster synchrotron source could explain the reduced SZ decrement. The main problem here is that non-thermal electrons would not give a good fit to the X-ray data which are usually well fitted by thermal bremsstrahlung, although Lieu & Quenby (2006) also noted that the soft X-ray excess seen in the central regions of some clusters may be indicative of a significant embedded non-thermal X-ray component there.

Fosalba, Gaztañaga & Castander (2003) have discussed whether the Integrated Sachs–Wolfe (ISW) effect could mask the SZ effect but the ISW effect is at 0.5 μK and seems too small to mask the SZ effect which in the X-ray clusters can be 10× higher.

There is also the possibility that the SZ decrement has been overestimated by the X-ray modelling. Certainly the *Chandra* predicted decrements for the five clusters in common with the *ROSAT* sample (A665, A1 413, A1 689, A1 914, A2 218) are on average ≈80 per cent larger than the predicted decrements from the *ROSAT* data. Most of this difference arises from A2218 where the *ROSAT* data imply $\Delta T(0) = -0.27$ mK (corrected to 30 GHz) and the *Chandra* data imply $\Delta T(0) = -0.87$ mK, a factor of 3.2 different. But since *Chandra* has higher spatial resolution, it is expected to probe the central core of a cluster more accurately and so the *Chandra* X-ray models might be expected to be more robust than those from the *ROSAT* data.

While this paper was in preparation, Afshordi et al. (2006) have also used X-ray data of 193 Abell clusters to search for the SZ decrement from *WMAP*3 data (see also Afshordi, Lin & Sanderson 2005). These authors made a significant detection and also suggested that the size of SZ decrement implied that the cluster hot gas fraction was 32 ± 10 per cent lower than the baryon fraction in the standard cosmological model. They also suggested that their *WMAP* results were consistent with the interferometric SZ results for the sample of 38 *Chandra* clusters analysed above. Note that the approach of Afshordi et al. (2006) is different from that used here in that the X-ray data are mainly used to define a template to detect SZ decrements and then the SZ data and the X-ray temperature data alone are used to establish the gas densities. This route therefore avoids comparing the SZ results with X-ray gas density models on the grounds that the latter depend on assumptions such as that of hydrostatic equilibrium. These authors also do not consider the possibility that the cluster SZ decrements may evolve with redshift.

Finally, if we assume that the *WMAP* SZ decrements are reliable, even in the case of the 38 *Chandra* clusters where the unexplained discrepancy persists with the OVRO/BIMA results of Bonamente et al. (2006), we might speculate whether a lower than expected SZ decrement in the higher redshift clusters could be caused by foreground lensing. The indication from *WMAP* that the higher redshift clusters may have reduced SZ decrements is consistent with the idea that gravitational lensing is having a significant effect on the detection of the SZ effect. Therefore it may be that the groups and clusters out to redshifts in the range $0.2 < z < 0.8$ in the foreground of the targeted *Chandra* clusters are lensing the cluster centres and smoothing the decrement away. Using CMBFAST we have constructed the lensing smoothing function for CMB scattering at $z = 0.3$ and find that on the size of the ≈10 arcmin *WMAP* beam, the smoothing function is reduced by about a factor of ≈10 compared to the case where the surface of last scattering is at $z = 1100$. At $z = 0.7$, the factor is ≈5. Therefore for the standard model this would make the effect negligible because at $z = 0.3$, $\epsilon = \sigma/\theta \approx 0.004$ and at $z = 0.7, \epsilon = \sigma/\theta \approx 0.008$. Only if the mass power spectrum is significantly higher than that for the standard model can this explanation apply. One such case is the high-mass power spectrum advocated by Shanks (2007) as a route to modify the first acoustic peak in the CMB. Such a spectrum is motivated by the evidence from QSO lensing that the galaxy distribution is strongly antibiased ($b \approx 0.1$) at least on 0.1–1 $\rm h^{-1}$ Mpc scales with respect to the mass (Myers et al. 2003, 2005; Mountrichas & Shanks 2007). However, the balance of other evidence may still argue against such a high amplitude for the mass power spectrum.

Lensing would clearly also affect the X-ray cluster profiles as well as the SZ decrements. Although these are expected to be smoother than the SZ decrements, it might be expected that the profiles of lower redshift clusters are on average steeper than the profiles of higher redshift clusters. It remains to be seen whether this prediction of the lensing hypothesis can be decoupled from evolution of the cluster gas component. In any case, the flatness of the X-ray profiles towards the centres of many clusters may make this prediction more difficult to test.

7 CONCLUSIONS

We have confirmed the extended appearance of the SZ decrement in *WMAP* 3-yr data around ACO $R \geqslant 2$ clusters out to $\theta \approx 30$ arcmin, first shown by Myers et al. (2004) using *WMAP* 1-yr data. Further to this, we have confirmed the detection of the SZ decrement in the 3-yr data around clusters identified in both the APM survey and 2MASS, showing an increase in detection significance compared to the 1-yr data analysis.

We have also confirmed the result of Lieu et al. (2006) that the SZ decrement is somewhat lower than expected on standard model assumptions and *ROSAT* X-ray profiles for a sample of 31 clusters from Bonamente et al. (2002). We have further shown that even smaller X-ray decrements are seen in the higher redshift sample of 38 clusters of Bonamente et al. (2006) that has *Chandra* X-ray data. The reason for the observational discrepancy between the *WMAP* data and the BIMA/OVRO data of Bonamente et al. (2006) is not clear. We do not believe that discrete or diffuse cluster radio sources nor the ISW effect is likely to explain the discrepancy. Dividing the ACO clusters into high- and low-redshift samples also indicates that the deficit in the SZ decrement may increase at higher redshift.

In the light of the above results from our *WMAP* SZ analysis, we have discussed the possibility that the extended SZ signal detected for ACO and 2MASS clusters may actually be indicating a lack of SZ signal in the centres of clusters rather than an excess at the edges.

On the assumption that the *WMAP* SZ results are correct, one explanation we have considered is that lensing of the cluster centres by foreground groups and clusters could explain the overprediction of the observed decrements by SZ models and in particular the apparent tendency for higher redshift clusters to have smaller SZ decrements. However, before considering such interpretations further, we need to clarify if this is a real observational discrepancy between the OVRO/BIMA data and *WMAP*.

It will clearly be interesting to see if these *WMAP* results are confirmed in the higher resolution SZ observations made using the *Planck* satellite.

ACKNOWLEDGMENTS

We thank R. Lieu, N. Afshordi, M. Bonamente, W. Frith, G. Hinshaw and J. Mittaz for useful discussions. RMB acknowledges receipt of a PPARC PhD studentship.

REFERENCES

Abell G. O., Corwin H., Olowin R., 1989, ApJS, 70, 1
Afshordi N., Lin Y.-T., Sanderson A. J. R., 2005, ApJ, 629, 1
Afshordi N., Lin Y.-T., Nagai D., Sanderson A. J. R., 2007, MNRAS, 378, 293
Bennett C. L. et al., 2003, ApJS, 148, 97
Bonamente M., Lieu R., Joy M. K., Nevalainen J. H., 2002, ApJ, 576, 688
Bonamente M., Joy M. K., LaRoque S. J., Carlstrom J. E., Reese E. D., Dawson K. S., 2006, ApJ, 647, 25
Coble K., Carlstrom J. E., Bonamente M., Dawson K., Holzapfel W., Joy M., LaRoque S., Reese E. D., 2007, AJ, 134, 897
Fosalba P., Gaztañaga E., Castander F. J., 2003, ApJ, 597, L89
Hinshaw G. et al., 2003, ApJS, 148, 63
Hinshaw G. et al., 2007, ApJS, 170, 288
Huffenberger K. M., Seljak U., Makarov A., 2004, Phys. Rev. D, 70, 063002
Jarrett T. H., Chester T., Cutri R., Schneider S., Skrutskie M., Huchra J. P., 2000, AJ, 119, 2498
Lieu R., Quenby J., 2006, ApJ, preprint (astro-ph/0607304)
Lieu R., Mittaz J. P. D., Zhang S.-N., 2006, ApJ, 648, L176
Lin Y.-T., Mohr J. J., 2007, ApJS, 170, 71
Maddox S. J., Efstathiou G., Sutherland W. J., Loveday J., 1990, MNRAS, 243, 692
Mountrichas G., Shanks T., 2007, MNRAS, 380, 113
Myers A. D., Outram P. J., Shanks T., Boyle B. J., Croom S. M., Loaring N. S., Miller L., Smith R. J., 2003, MNRAS, 342, 467
Myers A. D., Shanks T., Outram P. J., Frith W. J., Wolfendale A. W., 2004, MNRAS, 347, L67
Myers A. D., Outram P. J., Shanks T., Boyle B. J., Croom S. M., Loaring N. S., Miller L., Smith R. J., 2005, MNRAS, 359, 741
Nevalainen J., Lieu R., Bonamente M., Lumb D., 2003, ApJ, 584, 716
Reiprich T. H., Böhringer H., 2002, ApJ, 567, 716
Shanks T., 2007, MNRAS, 376, 173
Sunyaev R. A., Zel'dovich Y. B., 1980, ARA&A, 18, 537

This paper has been typeset from a TEX/LATEX file prepared by the author.